General description of polarization in lidar using Stokes vectors and polar decomposition of Mueller matrices

Matthew Hayman,[1,*] Jeffrey P. Thayer,[2]

[1] *National Center for Atmospheric Research, Advanced Study Program, Boulder, CO, 80307, USA*

[2] *University of Colorado, Department of Aerospace Engineering Sciences, Boulder, Colorado, 80309, USA*

[*] *Corresponding author: mhayman@ucar.edu*

Polarization measurements have become nearly indispensible in lidar cloud and aerosol studies. Despite polarization's widespread use in lidar, its theoretical description has been widely varying in accuracy and completeness. Incomplete polarization lidar descriptions invariably result in poor accountability for scatterer properties and instrument effects, reducing data accuracy and disallowing the intercomparision of polarization lidar data between different systems. We introduce here the Stokes Vector Lidar Equation (SVLE) which is a full description of polarization in lidar from laser output to detector. We then interpret this theoretical description in the context of forward polar decomposition of Mueller matrices where distinct polarization attributes of diattenuation, retardance and depolarization are elucidated. This decomposition can be applied to scattering matrices, where volumes consisting of randomly oriented particles are strictly depolarizing, while oriented ice crystals can be diattenuating, retarding and depolarizing. For instrument effects we provide a description of how different polarization attributes will impact lidar measurements. This includes coupling effects due to retarding and depolarization attributes of the receiver which have no description in scalar descriptions of polarization lidar. We also describe how the effects of polarizance in the receiver can result in non-orthogonal polarization detection channels. This violates one of the most common assumptions in polarization lidar operation.

OCIS codes: 010.3640, 260.5430.

1. Introduction

Polarization lidar has long been used to characterize and study the thermodynamic phase, shape and composition of atmospheric aerosols and clouds [1–4]. It has been of common practice for systems to transmit a linearly polarized laser pulse into the atmosphere and segment the parallel and perpendicular planes of the backscattered light into two receiving channels via an analyzer. This lidar configuration has led to the widely used depolarization ratio, identified typically by the symbol δ, which is physically related to a particle's shape or thermodynamic phase under specific assumptions of the scattering matrix and system properties.

Although of significant value, the rather simplified approach of using the depolarization ratio to describe physical properties of the scatterer has often neglected the vector nature of light by replacing it with its approximate scalar counterpart with no physical construct [5]. Consequently complexities arise in the interpretation of measurements that cannot be adequately resolved by the imposed simplification. Without full specification of the lidar operation characteristics (transmit polarization, full description of measurement channels, specific polarization effects in the instrument, etc) and the scattering matrix under interrogation, the depolarization ratio data only indicates a change in polarization state. This leads to depolarization ratio estimates that are potentially contaminated or at least specific to the system, and limits the ability to examine the link between polarization and geographic location or meteorological season recorded by another polarization lidar [6].

Some work has addressed these issues by measuring full backscattered Stokes vectors [7, 8] while others have fully adopted a Mueller matrix description of scattering [5, 9–14]. To our knowledge, no end-to-end polarization theory has been presented as a baseline for polarization lidar design and analysis that provides a framework for more accurate and absolute estimates of scattering properties through polarization. Thus we introduce here the Stokes Vector Lidar Equation (SVLE), a fully general polarization description of lidar using Stokes vectors to represent the polarization state of light and Mueller matrices to describe the scatterer, instrument and transmission path.

Polar decomposition (PD) of Mueller matrices has successfully been used to help elucidate physical meaning from polarization measurements in characterization of silicon structures [16], monitoring changes in tissues [17], and detecting cancerous oral lesions [18]. Included in this work is a discussion on polarization effects described using forward-PD [15], their impacts, and how they are exhibited by atmospheric scatterers and the optical system. Two different scattering scenarios of randomly oriented and oriented atmospheric scatterers are investigated in this context to demonstrate the utility of the Stokes Vector Lidar Equation in interpreting the polarization measurements.

2. The Stokes Vector Lidar Equation

A complete description of polarization in lidar requires the use of conventional polarization theory as described in optics texts [19]. The light under consideration may be partially polarized and optical systems have the capability to change both the polarization state and degree-of-polarization (DOP) of the incident light. Thus, we use Stokes vectors to describe the polarization state of light. The general form for a Stokes vector is given by

$$\vec{S} = \begin{bmatrix} S_0 \\ S_1 \\ S_2 \\ S_3 \end{bmatrix}, \tag{1}$$

where S_0 is the total intensity of the light, S_1 is the difference in optical power between the horizontal and vertical modes, S_2 is the difference in optical power between the $\pm 45^\circ$ modes and S_3 is the is the difference in optical power between right and left hand circular polarizations modes. Alternatively, the same Stokes vector may also be written

$$\vec{S} = S_0 \begin{bmatrix} 1 \\ p\cos 2\psi \cos 2\chi \\ p\sin 2\psi \cos 2\chi \\ p\sin 2\chi \end{bmatrix}, \tag{2}$$

where ψ is the linear rotation angle of the polarization state, χ is the ellipticity angle of the polarization state, and p is the degree-of-polarization (DOP) which is the fraction of light that is polarized and often calculated

$$p = \frac{\sqrt{S_1^2 + S_2^2 + S_3^2}}{S_0}. \tag{3}$$

The generalization in Eq. (2) proves to be particularly useful for optimizing the transmitted polarization for specific optical systems or scattering problems. The projection of a normalized Stokes vector onto the Poincaré Sphere is shown as a function of the parameter definitions in Eq. (2) in Figure 1. The orientation of the Stokes vector in Poincaré space is given by the angle arguments 2ψ and 2χ, the sphere radius is 1 and the Stokes vector length is p.

Interactions along the optical path are described by Mueller matrices which may modify the light's polarization state and DOP. Thus, a complete description of polarization through a lidar system must be expressed in terms of Stokes vectors and Mueller matrices along the optical path. This description, which we call the Stokes Vector Lidar Equation (SVLE), can

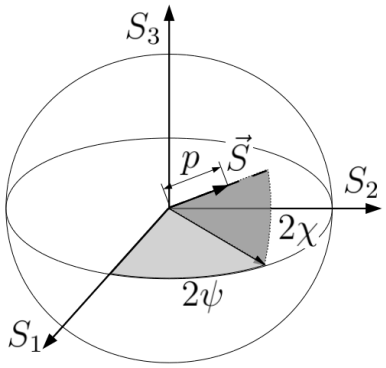

Fig. 1. Poincaré Sphere representation of a normalized Stokes vector. The sphere's radius is 1 and the Stokes vector length is the DOP p. The orientation of the Stokes vector is given by the rotation and ellipticity angles ψ and χ respectively. Linear polarizations are on the equator of the sphere and circular at the poles. Each meridian corresponds to a specific linear orientation. A Stokes vector of zero length (on the origin) is completely unpolarized.

be written as

$$\begin{aligned}\vec{S}_{RX}(R) = \; & \mathbf{M_{RX}}\left[\left(G(R)\frac{A}{R^2}\Delta R\right)\mathbf{T_{atm}}(\vec{k}_s,R)\right. \\ & \left.\times\mathbf{F}(\vec{k}_i,\vec{k}_s,R)\mathbf{T_{atm}}(\vec{k}_i,R)\mathbf{M_{TX}}\vec{S}_{TX}+\vec{S}_B\right].\end{aligned} \tag{4}$$

In Eq (4), $\vec{S}_{RX}$ is the received Stokes vector, $\vec{S}_{TX}$ is the Stokes vector describing the laser polarization state, $\mathbf{M_{TX}}$ is the Mueller matrix description of the transmitter and includes the polarization state generator, $\mathbf{T_{atm}}(\vec{k}_i,R)$ is the Mueller matrix description of the atmospheric transmission to the scatterer along incident wave vector $\vec{k}_i$ over the range R, $\mathbf{F}(\vec{k}_i,\vec{k}_s,R)$ is the scattering phase matrix (or Mueller matrix) of the scattering medium at range R for incident and scattered wave vectors $\vec{k}_i$ and $\vec{k}_s$ respectively, ΔR is the integration range bin, A is the collection aperture, *G(R)* is the geometrical overlap function, $\mathbf{M_{RX}}$ is the Mueller matrix description of the receiver, and $\vec{S}_B$ is the Stokes vector of the background at the input of the receiver. In all cases the average scattering and system efficiencies may be found in the (1,1) element of the respective Mueller matrix and intensity or photon counts is carried in the first element of the Stokes vector.

For simplicity, we assume in this work that $\mathbf{T_{atm}}$ may be represented by a scaled identity so that it has no impact on the transmitted polarization state. This is generally the case when interrogating single scattering [20] which is assumed throughout this work. This includes instances where single scattering observations are made through an optically dense layer [14].

It is important to note that for most polarization lidar, the scattering matrix is the term under investigation. The received Stokes vector is only an intermediary for analyzing the scattering medium. It is clear from Eq. (4) that we should select $\vec{S}_{TX}$ and measure $\vec{S}_{RX}$ in such a way to provide useful information about $\mathbf{F}(\vec{k}_i,\vec{k}_s,R)$. As such, any data products given through this analysis would be elements of the scattering phase matrix which is independent of instrument operation.

Even though $\mathbf{F}(\vec{k}_i,\vec{k}_s,R)$ is the target of characterization by the lidar system, it should be clear from Eq. (4) that the matrix probed by the transmit polarization is not strictly that of the scatterer. This configuration of polarization lidar can only probe the total product of all the Mueller matrices along the optical path. For this generalized description, one matrix cannot be isolated from the others, and the path must be evaluated as a whole.

The description provided in Eq. (4) relates the transmitted to received polarization through the lidar path. However, polarization cannot be directly measured and its characterization must consist of a series of inherently scalar measurements. Thus, the description of measurements performed by the lidar requires an additional operation. Generally this involves using an analyzer to project the received polarization onto an axis of the Poincaré Sphere and measure the resultant intensity. This process is described by an output matrix which relates the measured intensity or photon counts on the receiver channels to the received polarization.

$$\vec{N} = \mathbf{O}\vec{S}_{RX}, \tag{5}$$

where

$$\vec{N} = \begin{bmatrix} N_1 \\ N_2 \\ \vdots \end{bmatrix}, \tag{6}$$

and N_n is the photon counts on the *nth* channel and $\mathbf{O}$ is the output matrix corresponding to those measurements (generally analyzer/polarizer matrices) and written

$$\mathbf{O} = \mathbf{o}\begin{bmatrix} \mathbf{P_1} \\ \mathbf{P_2} \\ \vdots \end{bmatrix}, \tag{7}$$

where $\mathbf{P_n}$ is the *nth* projection matrix corresponding to the *nth* channel and

$$\mathbf{o} = \begin{bmatrix} \eta_1 & 0 & 0 & 0 & 0 & 0 & 0 & 0 & \\ 0 & 0 & 0 & 0 & \eta_2 & 0 & 0 & 0 & \cdots \\ & & & & \vdots & & & & \end{bmatrix}, \tag{8}$$

where η_n is the *nth* channel detector efficiency. This matrix $\mathbf{o}$ denotes that after projection, only the first element of the Stokes vector is measured. For N measurements, $\mathbf{o}$ is Nx4N. In the case of non-polarization backscatter lidar, $\mathbf{O}$ simplifies to $\begin{bmatrix} \eta & 0 & 0 & 0 \end{bmatrix}$.

For instances where the polarization lidar measures the parallel and perpendicular components of the backscattered light, $\vec{N}$ becomes

$$\vec{N} = \begin{bmatrix} N_{||} \\ N_{\perp} \end{bmatrix}, \tag{9}$$

and the output matrix is

$$\mathbf{O} = \mathbf{o}\begin{bmatrix} \mathbf{P}_{||} \\ \mathbf{P}_{\perp} \end{bmatrix} \tag{10}$$

where $\mathbf{P}_{||}$ and $\mathbf{P}_{\perp}$ are 4x4 Mueller matrix descriptions of parallel and perpendicular polarizers in the receiver respectively and $\mathbf{o}$ transforms the resulting eight element Stokes vector into the two measured photon counts,

$$\mathbf{o} = \begin{bmatrix} \eta_{D||} & 0 & 0 & 0 & 0 & 0 & 0 & 0 \\ 0 & 0 & 0 & 0 & \eta_{D\perp} & 0 & 0 & 0 \end{bmatrix}, \tag{11}$$

where $\eta_{D||}$ and $\eta_{D\perp}$ are the detector efficiencies of the parallel and perpendicular channels.

Thus the Stokes Vector Lidar Equation provides an end-to-end theoretically complete polarization description, giving full consideration to polarization effects in all components of the

optical path and how they impact the measurements of the lidar system. This analysis tool is critical for understanding the systematic error and measurement attributes of polarization lidar systems. Additionally, some non-polarization backscatter lidar systems may also need to perform this analysis if their measurements demonstrate polarization dependence [21].

3. Forward Polar Decomposition

Polar decomposition (PD) allows a Mueller matrix to be separated and represented as a product or sum of its fundamental physical polarization properties. Though there are many ways to perform and represent PD [22–25], we provide here an analysis of Mueller matrices in the context of forward-PD [15]. Through this analysis, a Mueller matrix can be decomposed into the product of three fundamental polarization effects: diattenuation, retardance and depolarization. The total Mueller matrix is the product of the matrices describing those effects.

$$\mathbf{M} = \mathbf{M}_\Delta \mathbf{M}_R \mathbf{M}_D, \tag{12}$$

where $\mathbf{M}$ is an arbitrary true Mueller matrix, $\mathbf{M}_\Delta$ is the depolarizing component of the Mueller matrix, $\mathbf{M}_R$ is the retarding component and $\mathbf{M}_D$ is the diattenuating component.

These three polarization effects are fundamentally unique in relation to each other. Thus approaches necessary to measure and account for them can also be quite different. We will provide a brief description of each effect here as it is important to understand the difference between some of these effects and their potential consequences in atmospheric lidar applications.

3.A. Diattenuator

A diattenuator is an optical element with polarization dependent efficiency and a corresponding preferential output polarization. In the context of polarization lidar, its presence in the scattering phase matrix means the volume scatters one polarization more strongly than another. In an optical system, its presence means the system has better transmission efficiency for one polarization than another.

A Diattenuator is fully described by transmission of unpolarized light T_u and its diattenuation vector $\vec{D}$, taking the form [15],

$$\mathbf{M}_D = T_u \begin{bmatrix} 1 & \vec{D}^T \\ \vec{P} & \mathbf{m}_D \end{bmatrix}, \tag{13}$$

where $\vec{D}$ is the 3 element diattenuation vector, and $\vec{P}$ is the polarizance which for a homogenous diattenuator $\vec{P} = \vec{D}$. The matrix $\mathbf{m}_D$ is a 3x3 submatrix fully described by the diattenuation vector through [15]

$$\mathbf{m}_D = \sqrt{1 - D^2}\mathbf{I} + \left(1 - \sqrt{1 - D^2}\right) \hat{D}\hat{D}^T, \tag{14}$$

where D is the magnitude of the diattenuation vector, $\hat{D}$ is the normalized diattenuation vector and $\mathbf{I}$ is a 3x3 identity matrix.

Due to their polarizance, diattenuators generally modify the polarization state of incident radiation, resulting in deformation of the Poincaré Sphere [26]. Outgoing polarizations will bend toward the polarizance vector in Poincaré space. This polarizance can also change the DOP of the incident radiation [27, 28].

Diattenuators are manifested in filters with non-normal incidence angles, folding mirrors, beam samplers and splitters, and polarizers. Though the diattenuation vectors of most individual optics in a lidar system are linear, the total system diattenuation vector may not correspond to linear polarizations.

3.B. Retarder

A retarder is a wave plate with an arbitrary fast axis that imposes a phase shift Γ between orthogonal polarization modes. This causes a rotation of the Stokes vector on the Poincaré sphere about the normalized retardance vector $\hat{R}$ [26]. For individual wave plates, $\hat{R}$ corresponds to linear polarizations, but in general this is not the case. The combination of two or more linear retarders generally result in a total $\hat{R}$ that corresponds to elliptical polarizations.

The retarder Mueller matrix takes the form [15]

$$\mathbf{M}_R = \begin{bmatrix} 1 & \vec{0}^T \\ \vec{0} & \mathbf{m}_R \end{bmatrix}, \tag{15}$$

where $\vec{0}$ is a three element zero vector and $\mathbf{m}_R$ is a 3x3 submatrix of $\mathbf{M}_R$ acting as a rotation matrix of angle Γ about the axis of its eigenvector $\hat{R}$.

In polarization lidar systems, retardance will modify the polarized state of incident light, but unlike the diattenuator, it will preserve the degree-of-polarization and orthogonality of polarizations states. Generally a retarder will convert linear polarizations into elliptical, making complete acceptance or rejection of polarization modes impossible with a linear polarizer.

Retardance commonly appears when lidar systems use folding mirrors. Newtonian telescopes are notorious for demonstrating this behavior due to the folding secondary mirror. Beam steering mirrors can also introduce retardance on the transmit side, resulting in elliptical transmit polarizations.

3.C. Depolarizer

Depolarizers are Mueller matrices describing nondeterministic polarization systems [29]. Included in the general set of these matrices are what we would more commonly think of as the depolarizers that decrease the degree-of-polarization of incident light. The most general form

of a depolarization matrix may exhibit polarizance. The most general form for a depolarizer is written [15]

$$\mathbf{M}_\Delta = \begin{bmatrix} 1 & \vec{0}^T \\ \vec{P} & \mathbf{m}_\Delta \end{bmatrix}, \tag{16}$$

where $\vec{P}$ is the polarizance vector describing the exit polarization state of unpolarized incident light and $\mathbf{m}_\Delta$ is a 3x3 submatrix of the matrix $\mathbf{M}_\Delta$. In the most general case, a depolarizer has nine independent terms. Three terms define the polarizance vector. Three define the depolarization or eigen values of the submatrix $\mathbf{m}_\Delta$. Finally three terms define the 3-dimensional orthonormal basis set of the depolarization terms or eigen vectors of $\mathbf{m}_\Delta$. Because the basis vectors of Poincaré space and $\mathbf{m}_\Delta$ are, by definition, linearly independent, there always exists some vector basis where $\mathbf{m}_\Delta$ may be diagonalized so that [30]

$$\mathbf{m}_\Delta = \mathbf{T}^{-1} \begin{bmatrix} 1-d_1 & 0 & 0 \\ 0 & 1-d_2 & 0 \\ 0 & 0 & 1-d_3 \end{bmatrix} \mathbf{T} \tag{17}$$

where d_n is the depolarization corresponding to the nth eigen vector of $\mathbf{m}_\Delta$ with $1-d_n$ as the corresponding eigen value of $\mathbf{m}_\Delta$ and $\mathbf{T}$ is the transformation matrix between the conventional S_1, S_2, S_3 coordinate system to the frame defined by the eigen vectors of $\mathbf{m}_\Delta$.

In Poincaré space the eigen values of $\mathbf{m}_\Delta$ shorten the incident Stokes vector while maintaining a constant radius on the sphere [28]. When all nonzero elements of $\mathbf{m}_\Delta$ on the diagonal are equal, the depolarizer is isotropic and the remaining outgoing polarized light maintains the same state as the input. However, more general anisotropic depolarization and the presence of polarizance $\vec{P}$ can cause the outgoing polarization state to change.

When diattenuation and retarding effects add incoherently, depolarization occurs. Thus, depolarizers exist as a result of averaging over randomness. These averages can include optical paths, particle orientation, size and shape and temporal variability of the optical path. While depolarizers are difficult to generalize, their presence often act as indicators about statistical variation in a sample volume.

Depolarization can exist in optical systems such as a receiver where mirrors reflect a range of incident angles. This range of angles results in variation of phase shift upon reflection, and the detected light will have a distribution of polarization states. In these cases, the total received Stokes vector is the sum of all individual Stokes vectors and the DOP will likely be reduced [31].

4. The Scattering Matrix

The types of polarization effects exhibited by a scattering volume are dictated by the distributions of size, shape, composition, orientation and symmetry of the particle species as

well as the lidar's polarization operation state. For purposes of this work, we generally assume particle symmetry and focus on orientation preference. We also only consider single scattering and assume the lidar is collecting backscattered radiation from a volume of such scatterers. While the SVLE does not require these assumptions, they greatly simplify the nature of scattering matrices which apply to most lidar applications.

4.A. Randomly Oriented Particles

The scattering phase matrix of randomly oriented, axially symmetric scatterers, have been reported in great detail [3,5,9,32]. Their backscatter phase matrix may be generally written

$$\mathbf{F}(\pi) = \beta \begin{bmatrix} 1 & 0 & 0 & 0 \\ 0 & 1-d & 0 & 0 \\ 0 & 0 & d-1 & 0 \\ 0 & 0 & 0 & 2d-1 \end{bmatrix}, \tag{18}$$

where β is the volume backscatter coefficient and d is referred to here as the depolarization of the scattering medium with allowable values between 0 and 1. If the incident polarization is linear, d is the fraction of polarized light that is depolarized by the scattering process. Note that the incident and scattered wave vectors have been replaced with the backscatter angle π. This is because the medium is macroscopically isotropic and its scattering properties are not a function of the specific direction of incidence.

The scattering matrix for randomly oriented axially symmetric particles shown in Eq. (18) is a pure depolarizer with no polarizance. The eigen vectors of $\mathbf{m}_\Delta$ align to S_1, S_2, and S_3. This matrix represents most common scattering cases in the atmosphere. The normalized matrix can be fully measured using conventional perpendicular/parallel polarization measurements that depend on the selected polarization of operation. For an arbitrary polarization, d may be calculated

$$d = \frac{4N_\perp}{\left(N_\perp + N_{||}\right)\left(3 - \cos 4\chi_L\right)}, \tag{19}$$

where $N_\perp$ is the signal measured on the polarization channel perpendicular to the transmit polarization, $N_{||}$ is the signal measured on the channel parallel to the transmit polarization and χ_L is the ellipticity angle of the transmitted and received polarizations (for linear polarizations $\chi_L = 0$ and circular polarizations $\chi_L = \pi/4$).

Note that the scattering matrix depolarizes circular polarizations more than linear. As a result, an arbitrary incident polarization will undergo a larger decrease in degree of circular polarization (DOCP) than degree of linear polarization (DOLP). For elliptical incident polarizations, the scattered polarized component will not be the same state as the incident polarized component. However for linear polarizations, (ignoring the π phase shift due to

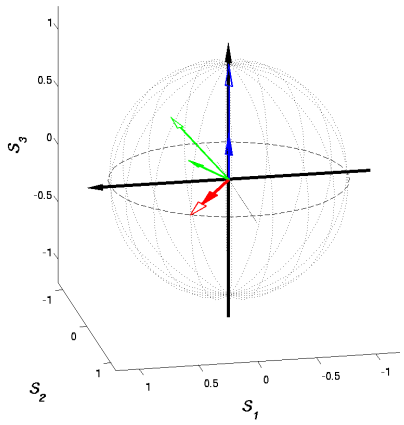

Fig. 2. (Color online) Poincaré Sphere representation of backscattered polarization states from random oriented scatterers with $d = 0.3$. The incident circular, linear and elliptical Stokes vectors (hollow blue, red and green respectively) are shortened after passing through the depolarizer (solid arrows of corresponding colors) while the sphere surface maintains constant radius. Totally linear or circular polarized input states have the same output polarized state, but circular components depolarize more than linear, so the elliptical polarization changes state. The π phase shifts usually associated with backscattering have been omitted for easier comparison of the incident and scattered Stokes vectors.

reversal of the wave vector) the polarized state will be preserved. Figure 2 shows how the scattered polarization states change for an incident elliptical, linear and circular polarization.

4.B. Oriented Particles

Unlike their randomly oriented counterparts, oriented scatterers may exhibit a variety of polarization effects under backscattering conditions. The backscatter matrix of horizontally oriented scatterers, such as those sometimes observed in cirrus clouds has the form [10, 32]

$$\mathbf{F}(\vec{k}_i, -\vec{k}_i) = \begin{bmatrix} f_{11} & f_{12} & 0 & 0 \\ f_{12} & f_{22} & 0 & 0 \\ 0 & 0 & f_{33} & f_{34} \\ 0 & 0 & -f_{34} & f_{44} \end{bmatrix}, \tag{20}$$

where the scattering medium is not macroscopically isotropic so the backscattering matrix is a function of the incident wave vector.

If we assume particles will orient within the horizontal plane and the lidar is pointing

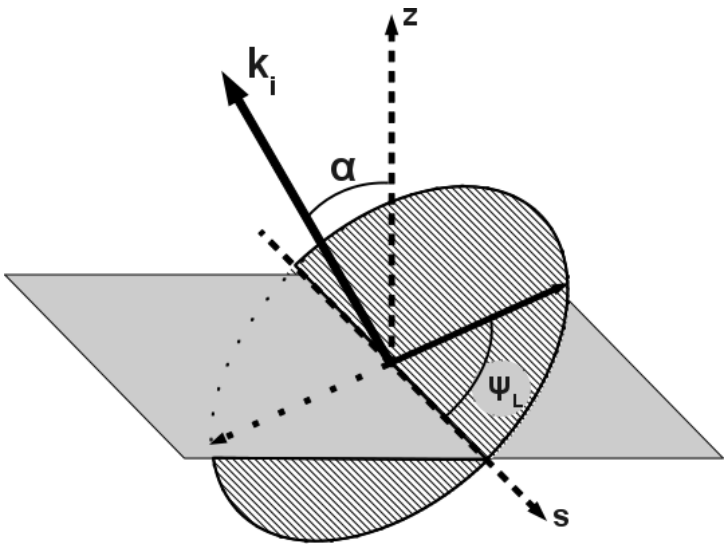

Fig. 3. Graphical depiction of angular terms for scatterers oriented in the horizontal plane. The lidar tilt angle α is measured relative to zenith (z axis) and the polarization angle ψ_L is measured relative to the linear polarization that lies in the horizontal plane (s axis).

along zenith/nadir ($\vec{k}_i$ is parallel to the vertical z-axis), scattering symmetry between all polarization planes gives a scattering matrix that simplifies to the depolarizing form in Eq. (18). In this case there is no distinction between the phase matrix form representing horizontally oriented and randomly oriented scatterers.

If the lidar does not point along zenith, diattenuating and retarding polarization effects will be exhibited based on the lidar/scatterer geometry. For a geometric representation of a tilted lidar with horizontally oriented scatterers, see Figure 3. The scatterers are aligned in the horizontal plane depicted. In this work, all linear polarization angles, ψ_L, are measured with reference to the s-polarization (the linear polarization that is in the horizontal plane). The directional cosine between the vertical z-axis and the incident wave vector $\vec{k}_i$ is the lidar tilt angle α.

With the scattering matrix expressed in Eq. (20), we assume that $\mathbf{T_{atm}}$, $\mathbf{M_{TX}}$ and $\mathbf{M_{RX}}$ are scaled identities and define $\vec{S}_{TX}$ using Eq. (2) with $\chi_L = \frac{\pi}{4}$ and $p = 1$. The detection polarization channels are described by perfect circular analyzers so the resulting measured circular depolarization ratio takes the form

$$\delta_c = \frac{f_{11} - f_{44}}{f_{11} + f_{44}}. \tag{21}$$

Applying the same assumptions as above, but now setting $\chi_L = 0$ and using linear ana-

lyzers in the receiver aligned to and orthogoanl to the transmitted polarization, we also find the linear depolarization ratio is given by

$$\delta_l = \frac{f_{11} - f_{22}\cos^2 2\psi_L - f_{33}\sin^2 2\psi_L}{f_{11} + 2f_{12}\cos 2\psi_L + f_{22}\cos^2 2\psi_L + f_{33}\sin^2 2\psi_L}, \tag{22}$$

where the quantity is a function of several elements in the phase matrix, and the transmitted polarization angle ψ_L.

Note that the linear depolarization ratio is a function of linear diattenuation (f_{12}) and possible retarding and depolarizing terms (f_{33} and f_{22}) [15]. Also, the circular polarization ratio may contain depolarizing and retarding terms (f_{44}). Thus, although δ contains the word "depolarization", in the case of oriented scatterers, it is not only related to the scatterer's effect on the DOP and may be a measure of a combination of diattenuation, retardance and depolarization.

A notable conclusion from Eq. (21) and (22) is that the depolarization ratio does not make any distinction between scattering matrix types. Nor can it distinguish polarization effects exhibited by the matrix. It only allows us to determine if the polarization changed. Where with randomly oriented scatterers, the depolarization ratio is only dependent on the ellipticity of the incident and detected polarizations, oriented scatterers also have dependence on the particular linear polarization plane, ψ_L. Though still useful, the depolarization ratio is an ambiguous (non-unique) term when the transmitted polarizations and form of the scattering phase matrix are not specified.

Oriented scatterers can also present an issue for non-polarization backscatter lidar. The meaning of backscatter measurements is not entirely clear when we consider diattenuating scatterers ($f_{12} \neq 0$), because the amount of light backscattered is a function of the transmitted polarization. The volume backscatter coefficient should be an intrinsic property of the medium and not a function of the instrument used to interrogate it. We use a convention where the volume backscatter coefficient is equal to the (1,1) element of the volume scattering phase matrix ($\beta = f_{11}$). However, if the lidar transmits linear polarization, the backscattered intensity or photon counts from a population of oriented ice crystals is not proportional to the volume backscatter coefficient

$$N_{RX} \propto f_{11} + f_{12}\cos 2\psi_L, \tag{23}$$

where N_{RX} is the received photon counts on the non-polarization backscatter lidar. Only if the transmit polarization is selected to be $\pm 45^\circ$ is the received photon count proportional to the volume backscatter coefficient.

Because of the different polarization effects exhibited by oriented scatterers, backscattered polarized components are generally not the same as the incident state. In Figure 4, we have plotted the same input polarizations used in Figure 2 with the resulting scattered Stokes

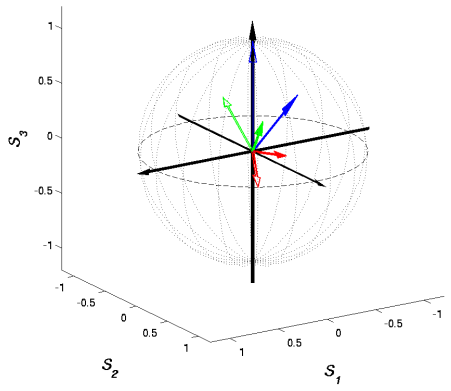

Fig. 4. (Color online) Poincaré Sphere representation of oriented scatterers with matrix given in [10]. The incident circular, arbitrary linear and arbitrary elliptical Stokes vectors (hollow blue, red and green respectively) are significantly changed after scattering (solid arrows of corresponding colors). Due to a combination of polarization effects, none of the scattered polarized states resemble the incident polarizations. The π phase shifts usually associated with backscattering have been omitted from this analysis.

vectors from an oriented scattering matrix. The matrix used in this example is reported in [10] as part of an "atypical but interesting case" and given as

$$\mathbf{F}(\vec{k}_i, -\vec{k}_i) = \begin{bmatrix} 1 & -0.51 & 0 & 0 \\ -0.51 & 0.89 & 0 & 0 \\ 0 & 0 & 0.513 & -0.08 \\ 0 & 0 & 0.08 & 0.40 \end{bmatrix} \tag{24}$$

The π phase shift resulting from the change in propagation direction has been removed for easier interpretation of the plot. Note that in this case, none of the input polarizations have the same polarized output. In all three input cases, polarizing, retarding and depolarizing effects in the scattering matrix result in elliptical, partially polarized output.

Unlike randomly oriented particles, the oriented backscatter matrix cannot be attributed to any single polarization effect. However, we can apply forward-PD to the matrix in Eq. (20) to determine how different polarization effects contribute to the scattering matrix terms [15]. The scattering phase matrix is composed of a combination of diattenuating, retarding and depolarizing terms

$$\mathbf{F}(\vec{k}_i, -\vec{k}_i) = f_{11}\mathbf{M}_{\Delta}^{F}\mathbf{M}_{R}^{F}\mathbf{M}_{D}^{F}, \tag{25}$$

where f_{11} denotes that all decomposed matrices are normalized and $\mathbf{M}_{\Delta}^{F}$, $\mathbf{M}_{R}^{F}$, and $\mathbf{M}_{D}^{F}$ are the depolarizing, retarding and diattenuating matrices of the backscatter phase matrix respectively. Comparing the form of the scattering matrix in Eq. (20) to that of a linear diattenuator and retarder, we see that the retarding and diattenuating axes are aligned (f_{12} corresponds to diattenuation between s- and p-polarizations, f_{34} corresponds to retardance between s- and p-polarization axes). Thus, by applying the matrix forms in Eq. (13) and (14), the scatterer diattenuation matrix is given by

$$\mathbf{M}_{D}^{F} = \begin{bmatrix} 1 & f'_{12} & 0 & 0 \\ f'_{12} & 1 & 0 & 0 \\ 0 & 0 & \sqrt{1 - {f'_{12}}^{2}} & 0 \\ 0 & 0 & 0 & \sqrt{1 - {f'_{12}}^{2}} \end{bmatrix}, \tag{26}$$

where f'_{12} is the normalized (1,2) element of the scattering matrix and also its diattenuation.

The retarder component of the scattering matrix is then given by the form of a linear wave plate aligned to s- and p-polarizations. The matrix evaluates to

$$\mathbf{M}_{R}^{F} = \begin{bmatrix} 1 & 0 & 0 & 0 \\ 0 & 1 & 0 & 0 \\ 0 & 0 & \cos\Gamma_{F} & -\sin\Gamma_{F} \\ 0 & 0 & \sin\Gamma_{F} & \cos\Gamma_{F} \end{bmatrix}, \tag{27}$$

where Γ_{F} is the phase shift imposed by the scatterer's retarding matrix.

The diattenuation and retardance matrix combine to define a homogeneous scattering matrix. In the presence of a single scatterer, there is no depolarizing effect. However, because the time averaged volume matrix is the sum of many scattering matrices, depolarizing effects must generally be included [33]. The depolarization matrix from Eq. (16) can be reduced to contain five terms. In order to maintain symmetry between the (1,2) and (2,1) terms in Eq. (20), polarizance must exist along s- or p-polarizations. This means the (2,1) element of the depolarization matrix is not generally zero. In Eq. (26), (27) and the total volume phase matrix in Eq. (20) there are no off diagonal terms coupling between the S_1 element and the other two Stokes vector elements. Thus, $\mathbf{M}_{\Delta}^{F}$ cannot contain any off diagonal terms coupling the s- and p-polarizations and the other two Stokes elements. As a result, $[\ 1 \quad 0 \quad 0\ ]^{T}$ must be an eigenvector of $\mathbf{m}_{\Delta}$. There is, however, cross coupling due to retardance between the circular and $\pm 45°$ Stokes vector terms. We must account for this to contribute to depolarization in the assumed form of the depolarization matrix. This results in symmetric, non-zero (3,4) and (4,3) elements in the depolarization matrix. Thus the general assumed form of the

depolarization matrix becomes

$$\mathbf{M}_{\Delta}^{F} = \begin{bmatrix} 1 & 0 & 0 & 0 \\ P_1 & 1-d_1 & 0 & 0 \\ 0 & 0 & 1-(d_3 - d_x\cos^2\theta_x) & \frac{d_x}{2}\sin 2\theta_x \\ 0 & 0 & \frac{d_x}{2}\sin 2\theta_x & 1-(d_2 + d_x\cos^2\theta_x) \end{bmatrix}, \tag{28}$$

where P_1 is the polarizance of the depolarization matrix along s- and p-polarizations, d_1 is the depolarization along s- and p-polarizations, d_2 is the depolarization along the eigenvector closest to $\pm 45°$, d_3 is the depolarization along the eigenvector closest to circular polarizations, and $2\theta_x$ is the angle in Poincaré space between the eigenvectors of $\mathbf{m}_{\Delta}$ and the S_2 and S_3 basis vectors. Thus when θ_x is not an integer multiple of $\pi/2$, there are off diagonal terms in $\mathbf{m}_{\Delta}^{F}$. Finally d_x is a depolarization cross talk term that is strictly a function of the other depolarizations and is given by

$$d_x = d_3 - d_2. \tag{29}$$

By evaluating Eq. (25) and imposing the symmetry requirement between the (1,2) and (2,1) elements exhibited by the total volume phase matrix in Eq. (20), we find the polarizance in Eq. (28) is not independent and is given as

$$P_1 = d_1 f'_{12}. \tag{30}$$

We then also apply the requirement for antisymmetry between the (3,4) and (4,3) elements ($f_{34} = -f_{43}$) shown in Eq. (20). This gives a simple relation between angle of the eigen axes in the depolarizer θ_x and the retardance of the scattering matrix Γ_F

$$\theta_x = \frac{\Gamma_F}{2}. \tag{31}$$

The volume scattering phase matrix given in Eq. (20) for oriented scatterers has six independent terms. Thus, forward-PD also gives six independent terms corresponding to physical polarization effects: f_{11} (related only to backscatter intensity), f'_{12} (diattenuation), Γ_F (retardance), d_1, d_2, and d_3 (all three: depolarization).

Though both realizations of the scattering phase matrix have six independent terms, the expression of these terms appear in different matrix elements, allowing us to isolate those polarization attributes we are interested in and offering greater flexibility in lidar operation. Also, PD terms are likely to be more physical in relation to relevant scatterer parameters [16,34]. Thus, we may not have to measure the complete phase matrix to determine a specific physical attribute of the volume.

5. Instrument Effects

The polarization matrices described in Section 3 can also be exhibited in optical systems where they generally corrupt and introduce error to the polarization lidar measurements. Error dependencies and successful error correction and calibration techniques will often be different with different polarization effects in both the scatterer and the instrument.

In the analysis introduced below, we will assume that all scattering volumes under interrogation are those of randomly oriented axially symmetric scatterers, so their scattering matrix is given by Eq. (18) [5,9]. We will assume that the transmit polarization is well known, and consider only polarization effects in the receiver.

5.A. Depolarization

Most depolarization effects in an optical system only decrease the DOP of received light. The presence of polarizance in an optical system will be discussed in detail with diattenuation. There are two potential cross talk effects from depolarizers. First, the depolarized component of light from the instrument will split evenly between all possible orthogonal polarizers, resulting in overestimates of depolarization. If there is no substantial diattenuation in the receiver system, this effect can be corrected using post processing error calibration and correction algorithms [35]. Also, when the depolarizer is anisotropic and its eigen vectors do not align to the polarizations of operation, the polarized state will change (as previously shown for randomly oriented scatterers in Figure 2).

As long as the transmitted and scattered polarization states do not change, depolarization can be corrected by realigning the polarizer in the receiver to the polarized state after the optical system. Presumably, this occurs in polarization optimization anyway, but it is important to note that systems which change the transmit polarization state may be susceptible to variable polarization coupling issues from anisotropic receiver depolarization. When altitudes of known depolarization exist in the recorded profiles, this effect can still be removed in data using post processing calibration and correction described in [35].

5.B. Retardance

An arbitrary retarder may be decomposed into a combination of linear retarder (a linear wave plate) and rotator [22, 36, 37]. The rotation effect of a system is rarely of concern, because presumably, the receiver polarizer angles are already optimized to best accept and reject the perpendicular and parallel polarizations based on atmospheric returns. The existence of linear retardance however presents an issue because it generally makes linear and circular polarizations elliptical. For linear polarizations, the resultant ellipticity angle is given [38]

$$\sin 2\chi = \sin 2\theta \sin \Gamma, \tag{32}$$

where χ is the ellipticity angle of the exit polarization, θ is the rotational angle between the incident polarization and retarder fast axis, and Γ is the retarder's phase shift. With the received polarization in an elliptical state, linear polarizers cannot be aligned to completely accept or reject the received light. Retarders do not change DOP, but the ellipticity of the received light will appear as such when observed in common two polarization measurement schemes. This apparent depolarization results in overestimation of atmospheric depolarization.

It is important to be aware that the resultant polarized output state of a retarder is dictated by the input supplied to it. Thus error from retarding effects measured at one polarization state is not necessarily a baseline minimum error. Error contributions can be avoided in lidar using linear polarizations by only operating in the polarization plane corresponding to the axis of the linear wave plate. The lidar's operation may either be rotated to this state using half wave plates, or the system's fast axis can be rotated to the lidar's plane of operation using a quarter wave plate. This fast axis is not necessarily an eigen polarization of the retarder. It is a polarization where a linear input polarization results in a linear output polarization (but not necessarily the same linear polarization). Hardware solutions also exist for lidars that transmit and receive multiple polarization states. A compensator composed of two quarter wave plates can be constructed as the inverse of the optical system's retarding matrix [39]. This allows operation in all polarizations without error contributions from retarding effects. Finally, if receiver diattenuation is not substantial, post processing error calibration and correction algorithms can also be used to remove retarding effects [35].

Thus retardance, though a common and significant error contributor to polarization lidar systems can be corrected and avoided using a variety of polarization correction schemes.

5.C. Diattenuation and Polarizance

In general we describe diattenuators as elements with polarization dependent efficiency. Thus, when diattenuation is present in the receiver, one polarization channel has a different efficiency than the other. This issue impacts backscatter lidar even if it does not analyze polarization [21]. In such cases, the polarized light will see one optical efficiency, while depolarized light will see another. Thus measured backscattered signal is dependent on the polarization properties of the scatterer. In the case of backscatter lidar the easiest way to make receiver throughput polarization independent is to transmit a linear polarization at 45° relative to (orthogonal in Poincaré space) the system's linear diattenuation vector. This removes any dependency on scatterer depolarization properties in the backscatter measurements.

Unlike the non-polarization lidar case, operating at 45° to the system diattenuation vector makes a poor solution in polarization lidar. Generally, aligning the polarization of operation to the diattenuation vector is the lesser of two evils where one channel's output must

be scaled by the difference in optical efficiencies. This is because a pure diattenuator also exhibits polarizance at the same orientation and magnitude as its diattenuation vector (for pure diattenuators $\vec{D} = \vec{P}$). This effect draws polarizations onto the polarizance vector. Because this operation is not a linear rotation, orthogonal polarizations will not remain so after passing through a matrix containing polarizance. The only exception to this is when the polarizations are aligned to, and directly orthogonal to (opposite in Poincaré space), the polarizance vector. If this condition is not met, two polarization channels that are by themselves orthogonal, may not appear orthogonal to backscattered light. That is, the polarization of maximum in transmission through one receiver polarization channel will not necessarily correspond to a minimum in transmission through the other.

This effect can be seen by multiplying a diattenuator matrix by the polarizer matrices of the two channels. If we assume the diattenuator is linear, its polarizance vector is

$$\vec{P}_{RX} = |\vec{P}_{RX}| \begin{bmatrix} \cos 2\theta_P \\ \sin 2\theta_P \\ 0 \end{bmatrix}, \tag{33}$$

where θ_P is the linear rotation angle of the polarizance vector relative to the parallel channel and $|\vec{P}_{RX}|$ is the magnitude of the polarizance vector. The diattenuation matrix of the optical system is then given by Eq. (13) when $\vec{D}_{RX} = \vec{P}_{RX}$. The total parallel analyzer, as it appears to the backscattered light before entering the receiver, is

$$\mathbf{M}_{D\parallel} = \mathbf{P}_{\parallel}\mathbf{M}_D(\theta_P, |\vec{P}_{RX}|), \tag{34}$$

where $\mathbf{P}_{\parallel}$ is a linear analyzer parallel to the transmit polarization, and the total perpendicular analyzer is

$$\mathbf{M}_{D\perp} = \mathbf{P}_{\perp}\mathbf{M}_D(\theta_P, |\vec{P}_{RX}|), \tag{35}$$

where $\mathbf{P}_{\perp}$ is a linear analyzer perpendicular to the transmit polarization. The angle between the polarizers performing the measurement can be determined using the dot product of their respective diattenuation vectors describing the two channels in Eq. (34) and (35)

$$\Delta\theta_{pol} = \frac{1}{2}\arccos\left(\hat{D}_{RX\perp} \cdot \hat{D}_{RX\parallel}\right), \tag{36}$$

where $\hat{D}_{RX\perp}$ is the normalized diattenuation vector of the perpendicular polarizer channel from Eq. (35), $\hat{D}_{RX\parallel}$ is the normalized diattenuation vector of the parallel polarizer channel from Eq. (34), and $\cdot$ is the vector dot product operation. Evaluating Eq. (36) using the results of Eq. (34) and (35) gives

$$\Delta\theta_{pol} = \frac{1}{2}\arccos\left(\frac{|\vec{P}_{RX}|^2\left(1+\sin^2 2\theta_P\right)-1}{1-|\vec{P}_{RX}|^2\cos^2 2\theta_P}\right). \tag{37}$$

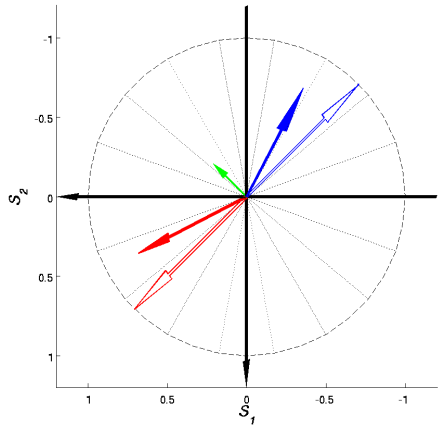

Fig. 5. (Color online) Poincaré Sphere representation of two orthogonal polarizations before (hollow red and blue) and after (solid red and blue) passing through a diattenuator with $|\vec{P}| = 0.3$. The polarizance vector is depicted as the solid green arrow. Though the two polarizations are orthogonal prior to the diattenuator, polarizance corrupts this relationship so they can no longer be perfectly separated using a polarizing beam splitter.

For truly orthogonal polarization channels, $\Delta\theta_{pol}$ is 90°, so the argument of the arccos should be -1. At a fixed polarizance magnitude $\Delta\theta_{pol}$ deviates the most from 90° when the polarizance vector is 45° (orthogonal in Poincaré space) to the polarization of operation. Note that in a pure diattenuator, this is also the polarization angle where backscatter intensity is no longer polarization dependent. In the case of polarization lidar, however, it is probably preferable to calibrate and correct polarization dependence in backscatter rather than attempt to correct for non-orthogonal polarization channels.

The effect of polarizance on orthogonal polarizations can be seen in Figure 5 where two orthogonal polarizations are passed through a diattenuator with polarizance $|\vec{P}| = 0.3$ oriented 45° relative to the input polarizations. After passing through the diattenuator, the polarizations are no longer orthogonal. Orthogonal backscattered polarizations are not orthogonal in the instrument, so a perfect polarizing beam splitter cannot isolate these modes.

We simulate a pure diattenuator in the receiver with fixed orientation angle of 45° to the lidar's parallel channel while allowing the magnitude of polarizance to vary. The polarization channels are set to be orthogonal by themselves (perfect polarizers set to 0° and 90°). The resulting apparent angle between the two polarization channels as seen by light before it enters the receiver is then plotted in Figure 6 as a function of polarizance magnitude.

Since nearly all polarization lidars assume that the parallel and perpendicular channels are

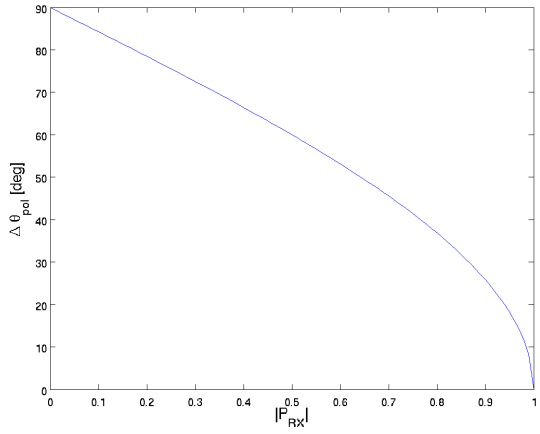

Fig. 6. Angle between orthogonal polarization channels as a function of polarizance magnitude when polarization analyzers are preceded by a pure diattenuator at 45° to the polarization of operation. The difference in analyzer angles is reported in degrees. Even small amounts of polarizance cause the optical system to violate the assumption that the two polarization channels are orthogonal.

orthogonal to each other, this polarization effect presents a significant concern. Clearly the greater the polarizance of the optical system, the less orthogonal the polarization channels become.

6. Conclusion

In todays modern lidar systems, a full polarization description of the instrument and its operation is needed for design, analysis and better understanding of the quantities under measurement. The introduction of additional channels, wavelengths and measurement techniques mean that nothing less than a fully general approach to polarization can provide the necessary analysis to understand the instruments capabilities and weaknesses. We have introduced here the Stokes Vector Lidar Equation (SVLE) to act as a theoretical basis for describing polarization in lidar. The polarized state of light is described using Stokes vectors and the polarization effects along the entire optical path are described using Mueller matrices. We have provided an introduction to interpretation of these Mueller matrices through forward polar decomposition, where any polarization effect may be exhibited in the atmosphere, scattering phase matrices, and optical system. This decomposition approach allows us to redefine matrices in terms of their fundamental polarization effects of retardance, depolarization and diattenuation. Each polarization effect has a unique impact on both data

products and error in lidar measurements. While some effects like retardance are generally quite easy to account for, diattenuation presents a significant issue, where minimization of differential efficiency in polarization channels results in maximizing the effects of polarizance. While we briefly discussed some solutions to these issues, each lidar design requires its own SVLE analysis to determine the optimal system configuration and baseline errors.

The forward-PD analysis was also applied to the scattering phase matrix for randomly oriented axially symmetric scatterers, which exhibit only depolarizing attributes, and horizontally oriented ice crystals, which exhibit all three polarization effects. We have shown that the general form of the scattering matrix for horizontally oriented ice crystals can be decomposed, allowing us to analyze each matrix element and determine what polarization effects it contains. Further study in these polarization attributes may allow us to better link particular polarization effects to physical properties of oriented scatterers. Through the SVLE we have related received lidar photon counts to vector relationships that account for polarization transformations throughout the atmospheric path and lidar optical system. This approach helps to clarify the physics behind polarization in lidar systems and can provide a framework to standardize polarization analysis and lead to further advancements in its application to atmospheric scatterers.

References

1. R. M. Schotland, K. Sassen, and R. J. Stone, "Observations by lidar of linear depolarization ratios by hydrometeors," J. Appl. Meteor. **10**, 1011–1017 (1971).
2. K. Sassen, "The polarization lidar technique for cloud research: a review and current assessment," Bull. Am. Meteorol. Soc. **72**, 1848–1866 (1991).
3. M. Mishchenko and J. Hovenier, "Depolarization of light backscattered by randomly oriented nonspherical particles," Opt. Lett. **20**, 1356–1358 (1995).
4. E. V. Browell, C. F. Butler, S. Ismail, P. A. Robinette, A. F. Carter, N. S. Higdon, O. B. Toon, M. R. Schoeberl, and A. F. Tuck, "Airborne lidar observations in the wintertime arctic stratosphere: Polar stratospheric clouds," Geophys. Res. Lett. **17**, 385–388 (1990).
5. G. Gimmestad, "Reexamination of depolarization in lidar measurements," Appl. Opt. **47**, 3795–3802 (2008).
6. E. J. Yorks, D. L. Hlavka, W. D. Hart, and M. J. McGill, "Statistics of cloud optical properties from airborne lidar measurements," J. Atmos. Oceanic Technol. **28**, 869–883 (2011).
7. J. D. Houston and A. I. Carswell, "Four-component polarization measurement of lidar atmospheric scattering," Appl. Opt. **17**, 614–620 (1978).
8. M. D. Gusta, E. Vallar, O. Riviere, F. Castagnoli, V. Venturi, and M. Morandi, "Use of polarimetric lidar for the study of oriented ice plates in clouds," Appl. Opt. **45**, 4878–

4887 (2006).

9. C. J. Flynn, A. Mendoza, Y. Zheng, and S. Mathur, "Novel polarization-sensitive micropulse lidar measurement technique," Opt. Express **15**, 2785–2790 (2007).
10. B. V. Kaul, I. V. Samokhvalov, and S. N. Volkov, "Investigating particle orientation in cirrus clouds by measuring backscattering phase matrices with lidar," Appl. Opt. **43**, 6620–6628 (2004).
11. G. G. Matvienko, I. V. Samokhvalov, and B. V. Kaul, "Research of the cirrus structure with a polarization lidar: parameters of particle orientation in crystal clouds," in Proc. SPIE **5571**, 393–400 (2004).
12. A. Ben-David, "Mueller matrices and information derived from linear polarization lidar measurements: theory," Appl. Opt. **37**, 2448–2463 (1998).
13. Y. Hu, P. Yang, B. Lin, G. Gibson, and C. Hostetler, "Discriminating between spherical and non-spherical scatterers," J. Quant. Spectrosc. Radiat. Transfer **79-80**, 757–764 (2004).
14. Y. You, G. W. Kattawar, P. Yang, Y. X. Hu, and B. A. Baum, "Sensitivity of depolarized lidar signals to cloud and aerosol particle properties," J. Quant. Spectrosc. Radiat. Transfer **100**, 470–482 (2006).
15. S. Y. Lu and R. A. Chipman, "Interpretation of mueller matrices based on polar decomposition," J. Opt. Soc. Am. A **13**, 1106–1113 (1996).
16. J. Sanz, J. Saiz, F. González, and F. Moreno, "Polar decomposition of the mueller matrix: a polarimetric rule of thumb for square-profile surface structure recognition," Appl. Opt. **50**, 3781–3788 (2011).
17. N. Ghosh, M. Wood, S. Li, R. Weisel, B. Wilson, R. Li, and I. Vitkin, "Mueller matrix decomposition for polarized light assessment of biological tissues," J. Biophoton. **2**, 145–156 (2009).
18. J. Chung, W. Jung, M. Hammer-Wilson, P.Wilder-Smith, and Z. Chen, "Use of polar decomposition for the diagnosis of oral precancer," Appl. Opt. **46**, 3038–3045 (2007).
19. M. Borne and E. Wolf, *Principles of Optics* (University, 1999), 6th ed.
20. B. V. Kaul, "Lidar equation for the case of sensing optically anisotropic media," in Proc. SPIE **3495**, 332–339 (1998).
21. I. Mattis, M. Tesche, M. Grein, V. Freudenthaler, and D. Müller, "Systematic error of lidar profiles caused by a polarization-dependent receiver transmission: quantification and error correction scheme," Appl. Opt. **48**, 2742–2751 (2009).
22. J. Gil and E. Bernabéu, "Obtainment of the polarizing and retardation parameters of a non-depolarizing optical system from its mueller matrix," Optik **76**, 67–71 (1987).
23. J. Gil, "Polarimetric characterization of light and media," Eur. Phys. J. Appl. Phys. **40**, 1–47 (2007).

24. R. Ossikovski, A. Martino, and S. Guyot, "Forward and reverse product decompositions of depolarizing mueller matrices," Opt. Lett. **32**, 689–691 (2007).
25. M. Anastasiadou, S. Hatit, R. Ossikovski, S. Guyot, and A. Martino, "Experimental validation of the reverse polar decomposition of depolarizing mueller matrices," J. Eur. Opt. Soc. Rapid Publ. **2**, 07018-1-07018-7 (2007).
26. C. Ferreira, I. S. José, J. J. Gil, and J. M. Correas, "Geometric modelling of polarimetric transformations," Monografías del seminario Matemático García de Galdeano **33**, 115–119 (2006).
27. T. Tudor and V. Manea, "Ellipsoid of the polarization degree: a vectorial, pure operatorial Pauli algebraic approach," JOSA B **28**, 596–601 (2011).
28. B. DeBoo, J. Sasian, and R. Chipman, "Degree of polarization surface and maps for analysis of depolarization," Opt. Express **12**, 4941–4958 (2004).
29. R. Simon, "Nondepolarizing systems and degree of polarization," Opt. Comm. **77**, 349–354 (1990).
30. G. Strang, *Linear Algebra and Its Applications* (Thomson Learning, 1988), 3rd ed.
31. R. A. Chipman, "Mechanics of polarization ray tracing," Optical Engineering **34**, 1636–1645 (1995).
32. H. van de Hulst, *Light Scattering by Small Particles* (Wiley, 1981).
33. M. I. Mishchenko, "Light scattering by randomly oriented axially symmetric particles," JOSA A, **8**, 871–882 (1991).
34. J. Sanz, P. Albella, F. Moreno, J. Saiz, and F. González, "Application of the polar decomposition to light scattering particle systems," J. Quant. Spectrosc. Radiat. Transfer **110**, 1369–1374 (2009).
35. M. Hayman and J. Thayer, "Explicit description of polarization coupling in lidar applications," Opt. Lett. **34**, 611–613 (2009).
36. R. Simon and N. Mukunda, "Minimal three-component su(2) gadget for polarization optics," Phys. Lett. A **143**, 165–169 (1990).
37. V. Bagini, R. Borghi, F. Gori, M. Santarsiero, F. Frezza, G. Schettini, and G. S. Spagnolo, "The Simon-Mukunda polarization gadget," Eur. J. Phys. **17**, 279–284 (1996).
38. D. H. Goldstein, *Polarized Light* (Marcel Dekker, Inc., 2003), 2nd ed.
39. M. Hayman and J. Thayer, "Lidar polarization measurements of PMCs," J. Atmos. Sol. Terr. Phys. pp. 2110–2117 (2011).